Vietnam Journal of Earth Sciences 36 (2014) 470-479

(VAST)

Vietnam Academy of Science and Technology

Vietnam Journal of Earth Sciences

Website: http://www.vjs.ac.vn/index.php/jse

Simulation of long-term variations of the F2-layercritical frequency f_0F_2 at the northern tropical crest of ionization at Phu Thuy, Hanoi, Vietnam using the thermosphere-ionosphere-electrodynamics general circulation model (TIE-GCM)

Pham Thi Thu Hong*[1], C. Amory-Mazaudier[2,3], Le Huy Minh[1]

[1]*Institute of Geophysics, Vietnam Academy of Science and Technology, Hanoi, Vietnam*

[2] *Sorbonne Paris, UPMC University Paris VI, LPP, 4 place Jussieu 75252 Paris*

[3]*T/ICT4D, ICTP, Strada Costiera 11, I - 34151 Trieste Italy*

Accepted 27 December 2014

ABSTRACT

In this work, the long-term variations of the simulated f_0F_2 by the NCAR thermosphere ionosphere-electrodynamics general circulation model (TIE-GCM) at the northern tropical crest of ionization at Phu Thuy, Hanoi, Vietnam (geographic latitudes 21.03^{0}N and longitude: 105.95^{0}E) during the period from 1962 to 2002 are examined to evaluate the ability of this model to reproduce the major features of the f_0F_2 as observed. The TIE-GCM simulates the influences of migrating and non-migrating diurnal and semidiurnal tides at the lower thermosphere, and changes of geomagnetic activity on the long-term variations of the f_0F_2. It reproduces well the diurnal and seasonal variations. We analyze the diurnal and seasonal variations of the observed f_0F_2 at Phu Thuy in approximately the same solar activity condition as in 1964, 1996 for the March and September equinoxes and June and December solstices. The local time and seasonal structures of these simulated results correspond well to those that are observed in 1964. On the contrary, the TIE-GCM does not reproduce the amplitude observed at Phu Thuy in 1996. The TIE-GCM with the chosen inputs does not yet allow us to explain well the long-term variations observed at Phu Thuy. We also try the different numerical simulations to understand how the long-term variations of the f_0F_2 is formed, how it relates to the current global system and its relationship with the thermosphere wind. The simulations show that the calculated NmF2 values are lower than the observed values. We find that the modeled contributions of the migrating and non-migrating diurnal and semidiurnal tides may cause them to play a major role in reducing the amplitude of the NmF2. The contributions of the integrated hemispheric power of auroral electrons and the cross polar cap potential seem to play an important role in increasing the amplitude of the NmF2.

Keywords: Ionosphere, foF2, long-term variations, modelling, geomagnetic field.

1. Introduction

Trends in ionospheric parameters have become a main subject since the beginning of the 1990’s (Aikin, 1991; Jarvis, et al., 1998; Roble, 1995; Ulich and Turunen, 1997). Clilverd et al. (1998) and Stamper et al. (1999) found that the geomagnetic activity in terms of the aa-index was increasing throughout the 20th century, and Clilverd et al. (1998) also found that the number of geomagnetic storms per solar cycle had also

*Corresponding author, Email: hongnd76@yahoo.com

been increasing until it stabilized in the last few cycles. Long-term changes in the solar quiet-time day variation, S_q, have been found as well (Elias, A.G. et al., 2010; Macmillan, S. et al., 2007). Variations I geomagnetic activity occur on short timescales from minutes to days, and are responsible for a part of the large natural variability in the thermosphere-ionosphere system. A gradual, long-term change in the background level of geomagnetic activity could therefore cause a long-term trend in the upper atmosphere (Cnossen et al., 2011). Hagan and Forbes (2002, 2003) found that the long-term changes in non-migrating tides (DE3) originated in the troposphere and propagating upwards has a strong influence on the ionosphere and thermosphere, especially at low latitudes. The long-term changes in the lower atmosphere therefore have the potential to induce long-term changes in the upper atmosphere. Quian and Burns (2009) performed a numeric simulation with the Thermosphere - Ionosphere-Electrodynamics General Circulation Model (TIE-GCM; (Richmond, et al.,1992)), focusing more on the effects of cooling of the F2-layer due to CO_2. They doubled the CO_2 concentration from 365 ppmv to 730 ppmv and noted the changes in the maximum of electron density in the F2-layer (NmF2) and the height peak in the F2-layer (hmF2), indicating the role of electrodynamics in long-term changes. From these results we can conclude that the change in CO_2 concentration has contributed to long-term trends in the F2-layer, but it is unlikely to be the unique cause.

The TIE-GCM of the National Center for Atmospheric Research (NCAR) is a three-dimensional model of general circulation, which take into account the energetic, chemical, dynamic and electrodynamics processes of the global thermosphere-ionosphere system between about 97 km and 500 km altitude, and allows us to identify the different parameters: components, density, temperature and velocities of ions and of neutral particles. Its inputs include solar ultraviolet radiation flux, parameterized by the F10.7 index, and upward propagating atmospheric tides at the lower boundary. As boundary conditions for the middle and upper atmosphere, the TIE-GCM uses a lower boundary tidal forcing from the Global Scale Wave Model (GSWM; (Hagan and Forbes, 2002, 2003). This model generates the influences of migrating diurnal and semi diurnal tides in the lower thermosphere about 97km through upwardly propagating, which includes only latent heat release as a source of non-migrating tides. At the upper boundary, approximately 500-600 km, the vertical O^+ flux is used, which approximates the plasma exchange between ionosphere and plasmasphere. In the polar cap, the electric potential distribution is described by the model of Heelis et al. (1982). In the low latitude region the geomagnetic field lines are assumed to be equipotential, which results in a symmetric electric potential about the geomagnetic equator.

The main purpose of this paper is to study the long-term variations of the critical frequency of the F2-region, f_0F_2 observed at Phu Thuy, Vietnam, presented by Pham et al. (Pham Thi Thu H. et al., 2011) using the TIE-GCM. We evaluate how well the TIE-GCM accounts for the long-term variations of the observed f_0F_2 at Phu Thuy during the period from 1962 to 2002, using the simulations of long-term variations of f_0F_2 that include the influences of migrating and non-migrating diurnal and semidiurnal tides at the lower atmosphere, and changes of geomagnetic activity, in order to determine their roles on long-term variations of the f_0F_2. We choose the solar minimum years in the series of observed data for the simulations. The estimates of trends caused by each of the mechanisms determined from these simulations are compared to observed trends.

2. Data and TIE-GCM calculation of maximum electron density

The hourly mean data of the critical frequency f_0F_2 of the ionospheric layer F2 recorded by the ionosonde at Phu Thuy observatory in the minimum solar years 1964 and 1996 for the March and September equinoxes and June and December solstices were analyzed. This observatory is located near the crest of equatorial anomaly (21.03°N, 105.96°E) in the Asian sector. The ionosonde data were continuously recorded by three different ionospheric vertical sounders: the IRX-Hungarian (1962-1966), the AIC-Russian (1967-1994), the IPS71-Australian (1994-2002).

The model inputs include solar ultraviolet radiation flux intensity, parameterized by the F10.7 index, integrated hemispheric power of auroral electrons, cross polar cap potential and migrating and "non-migrating" tidal components. The calculated parameter by the model is f_0F_2 in MHz, which is directly related to the peak electron density NmF2 in e/cm^3 (Rishbeth and Garriott, 1969) as:

$$N_mF_2 = 1.24\times10^{10}\left(f_0F_2\right)^2 \qquad (1)$$

The study is performed for the some different numerical simulations listed in Table 1.

Table 1. The different simulations

Simulations	Model inputs				
	F10.7 (sfu, 10^{-22} Wm^{-2} Hz^{-1})	Integrated hermispheric power of auroral electrons	Cross polar cap potential	Migrating diurnal and semidiurnal tides	Migrating and non-migrating tides
N^{0}1 (quiet) (Menvielle et al., 1992, 2006, 2011)	solar minimum, am<20nT	solar minimum, am<20nT	solar minimum, am<20nT	solar minimum, am<20nT	
N^{0}2 (quiet)	solar minimum, am<20nT	solar minimum, am<20nT	solar minimum, am<20nT	0	0
N^{0}3 (quiet)	70sfu	18GW	30kV	solar minimum, am<20nT	
N^{0}4 (quiet)	solar minimum, am<20nT	solar minimum, am<20nT	solar minimum, am<20nT		solar minimum, am<20nT
N^{0}5 (quiet)	solar minimum, am<20nT	1 GW	1 GW		solar minimum, am<20nT
N^{0}6 (perturbation)	solar minimum, am>20nT	solar minimum, am>20nT	solar minimum, am>20nT	solar minimum, am>20nT	

We focus on simulations of the diurnal variations of the NmF2 for the March and September equinoxes, and the December and June solstices, for mentioned above different conditions of the TIE-GCM during the solar minimum years (1964 and 1996). We then compare the results of these simulations with observations at Phu Thuy to evaluate the ability of the TIE-GCM to reproduce the morphological characteristics of the observations, it is the evolution between 1964 and 1996.

3. Model results and comparison to observations

3.1. Simulation of migrating tides

To study the tidal migration influences on the long-term variations of the critical frequency foF2, a simulation using the TIE-GCM has been executed with the first standard conditions including a tidal forcing at the lower boundary from the GSWM and the second condition removing the tidal forcing.

The first numerical simulation allows us to calculate the diurnal variation of the F2-layer maximum density, NmF2: the tidal migration influences on the NmF2 (blue curves), the second one does without the tidal migration influences (violet curves). The third simulation allows to calculate the diurnal variation of NmF2 under the influences of migrating tides, the integrated hemispheric power of auroral electrons and the cross polar potential on the diurnal variation of NmF2 (yellow curves).

Figure 1 shows the local time variations of the simulated NmF2 at Phu Thuy in March and September equinoxes, in June and December solstices, superimposed to the corresponding seasonal averaged observations for the solar minimum of 1964. This figure shows the consistency of the diurnal variations of TIE-GCM simulated NmF2 with observations. Indeed, the diurnal variation of NmF2 presents the expected shape, including the amplitude variation. The minimum amplitude of the observations at about 04.00 LT or 05.00 LT is well represented with the simulation results. The maximum amplitude of the observed NmF2 at Phu Thuy (red curves) at about 14.00 LT or 15.00 LT is always greater than the one of the simulated NmF2.

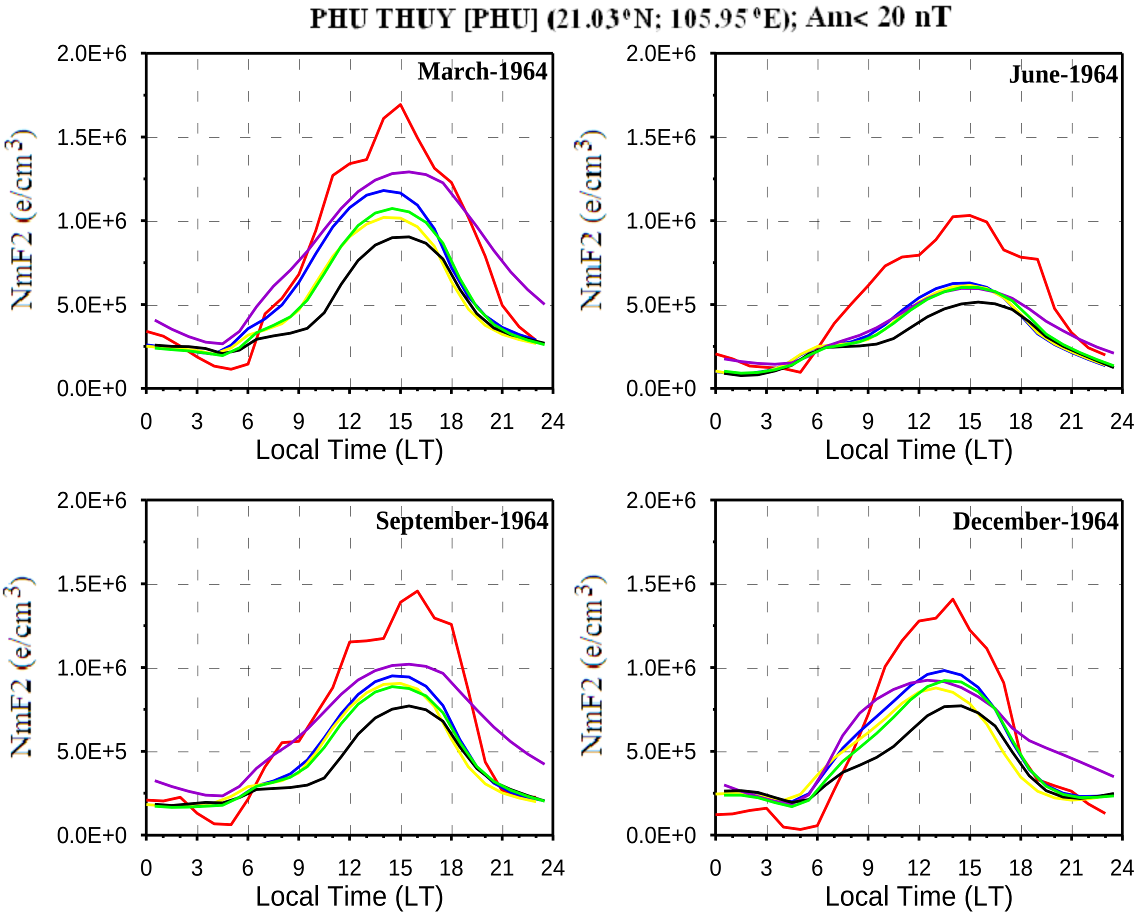

Figure 1. The diurnal variation of NmF2 at equinoxes and solstices. The red curves (--) are observed values at Phu Thuy in 1964. The blue curves (--) represent tidal migration influences (simulation N^{0}1), the green curves (--) migrating and non-migrating tides (simulation N^{0}4), the violet curves (--) without tidal migrating influences (simulation N^{0}2), the yellow curves (--) tidal migration influences with the F10.7 index (70sfu) (simulation N^{0}3), integrated hemispheric power of auroral electrons (18GW) and cross polar cap potential (30kV), and the black curves (--) migrating and non-migrating tides, integrated hemispheric power of auroral electrons (1GW), and cross polar cap potential (1kV) (simulation N^{0}5)

During equinoxes, the computed NmF2 amplitude is stronger than during solstices. The simulated amplitude of the violet curves (without atmospheric tides) is larger than the one of the yellow and blue curves (with atmospheric tides) during March and September; the violet curves are of the same amplitude as the blue curves in June. The amplitude of the blue curves (atmospheric tides) is stronger than the one of the yellow curves. This implies that the tidal influence is an important contribution to the seasonal variations of the NmF2, except in solstices. The green curves (migrating and non-migrating tides) are the same amplitude as the yellow curves in different seasons.

Figure 2 illustrates the seasonal variation of maximum ionization of the F2-layer, NmF2 observed at Phu Thuy and the simulated values with the TIE-GCM in the four seasons for the solar minimum of 1996.

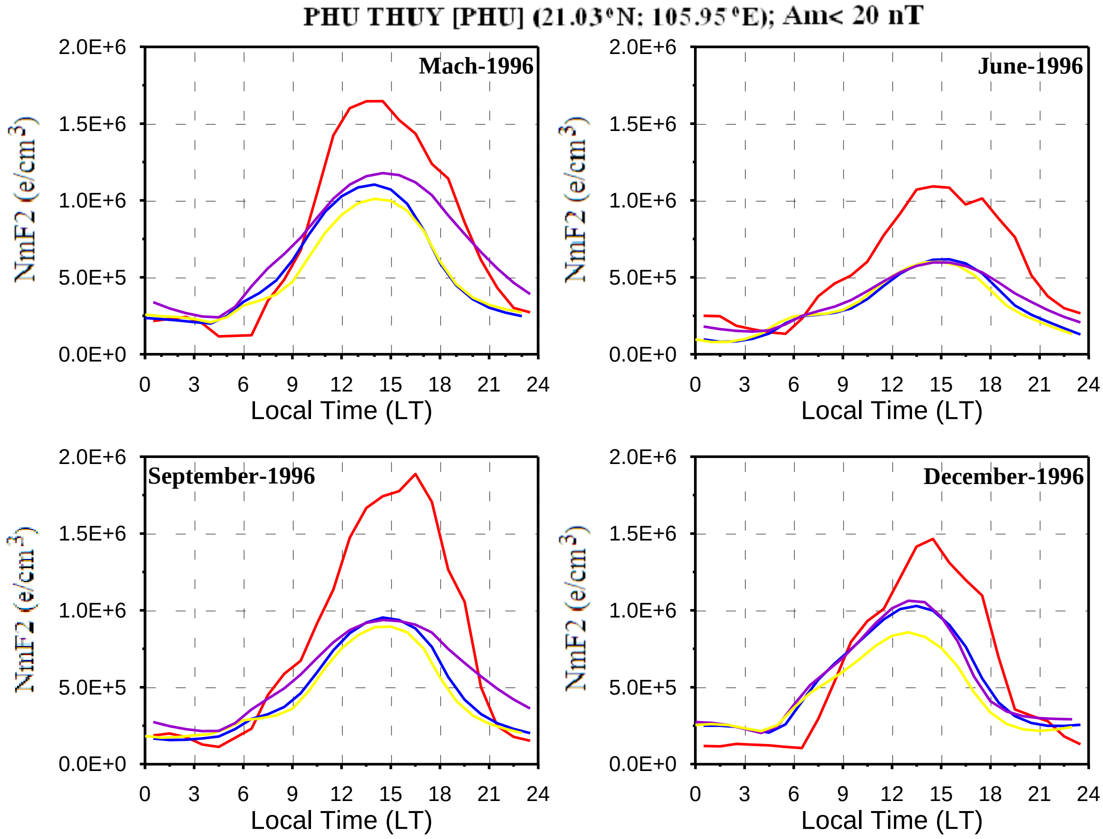

Figure 2. The diurnal variation de NmF2 at equinoxes and solstices. The red curves: seasonal averages of the observations at Phu Thuy in 1996, the blue curves represent tidal migration influences (simulation $N^0$1), the violet curves without tidal influences (simulation $N^0$2), and the yellow curves (simulation $N^0$3) tidal migration influences with integrated hemispheric power of auroral electrons (18GW) and cross polar potential (30kV) and F10.7 index (70)

We observe that the maximum amplitude of simulated diurnal variations at equinoxes and June solstice is usually different with one of the observed diurnal variations. The diurnal pattern in September equinox underestimates the value of observed NmF2. However, there is no difference between the simulated and observed shapes. The maximum amplitude at about 14.00 LT or 15.00 LT is higher in the observations than in the model. The most difference between the observations and the simulations is in the September equinox.

Figure 2 shows also that there is a little difference between the three simulations (simulation $N^0$1, simulation N^o2 and simulation $N^0$3) for the summer, autumn and winter. It is observed that the worst representation of observations is obtained when we introduce an electric potential on the polar cap (yellow curves), except in summer solstice.

3.2. Simulation of non-migrating tides (DE3) of the variation in long-term foF2

In this section, we consider the influences of non-migrating tides, originating in the troposphere during meteorological storms. Any long-term changes in the lower atmosphere have the potential to induce long-term changes in the upper atmosphere. We will study the influences of migrating and non-migrating tides in the region of Phu Thuy.

Figure 3 shows the diurnal variations of simulated NmF2 for the observatory Phu Thuy with or without the influences of the migrating and non-migrating tides (in simulations N^o2, N^o4 and N^o5) corresponding to observations at Phu Thuy for the four seasons in 1964. The calculated diurnal variations by the TIE-GCM are in reasonable agreement with the observations. Indeed, the minimum amplitudes of both simulations and observations are at about 04.00 LT or 05.00 LT in the morning. The maximum amplitudes at about 15.00 LT are greater in observations than in model at all seasons.

Figure 3 shows also the diurnal variations of simulated NmF2 as well as the results of three simulations. The green lines take into account the tidal influences, the violet lines are without tidal influences and the black lines include the tidal influences with the cross polar potential during the different seasons. The simulated amplitude is stronger in March and September (equinoxes) and weaker in December and June (solstices). The amplitudes of the violet lines are greater than ones of black and green in equinoxes. It shows that the influences of the tides and the cross polar potential have a non-negligible contribution to changes in NmF2 during equinoxes. In addition, the contribution of tides seems to play a major role in reducing the amplitude of NmF2. On the contrary, the contribution of the integrated hemispheric power of auroral electrons and of the cross polar potential seems to play a major role in increasing the amplitude of NmF2.

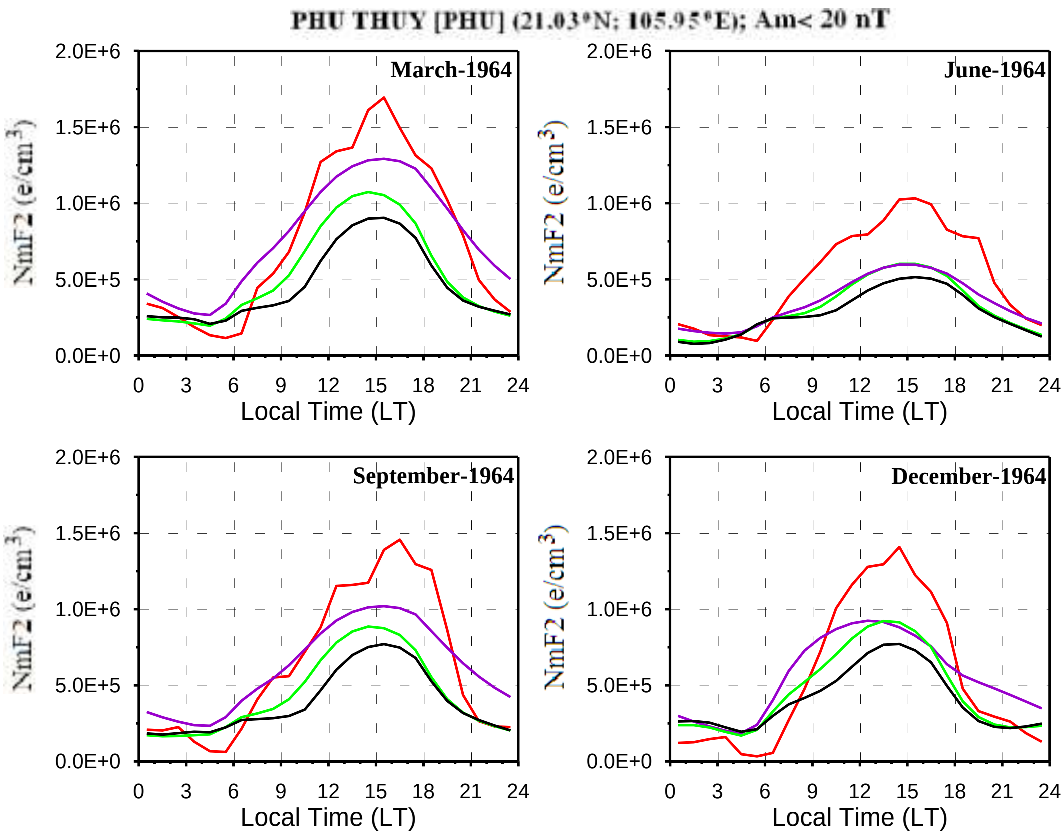

Figure 3. The diurnal variations of NmF2 at equinoxes and solstices. The red curves (--): seasonal averages of the observations at Phu Thuy in 1964, the green curves (--) represent the influences of the migrating and non-migrating tides, the violet curves (--) without the influences tides, and the black curves (--) influences of the migrating and non-migrating tides, the integrated hemispheric power of auroral electrons (1GW), and the cross polar cap potential (1kV)

Figure 4, similar to Figure 3, presents the diurnal variations of simulated NmF2 as a function of local time at Phu Thuy for the four seasons, and seasonal averages of the observations at Phu Thuy in 1996 in approximately the same conditions of Figure 3. Both the observations and simulations of the NmF2 have the same shape, and reach a minimum value at around 0500 LT. But the maximum amplitude of the modeled NmF2 at around 14.00 LT or 15.00 LT is less than the one of observed NmF2 for four seasons. The modeled maximum amplitude is smallest in summer and autumn equinox.

Figure 4 also shows that the simulated NmF2 variations in violet lines (without atmospheric tides) are greater than those in the green (with atmospheric tides) and black lines (with tidal influences + the cross polar potential), especially in spring. This shows that the tides, the integrated hemispheric power of auroral electrons, and the cross polar potential influence the variation of NmF2 in spring. The differences of amplitudes for the three simulations in summer, autumn and winter are negligible.

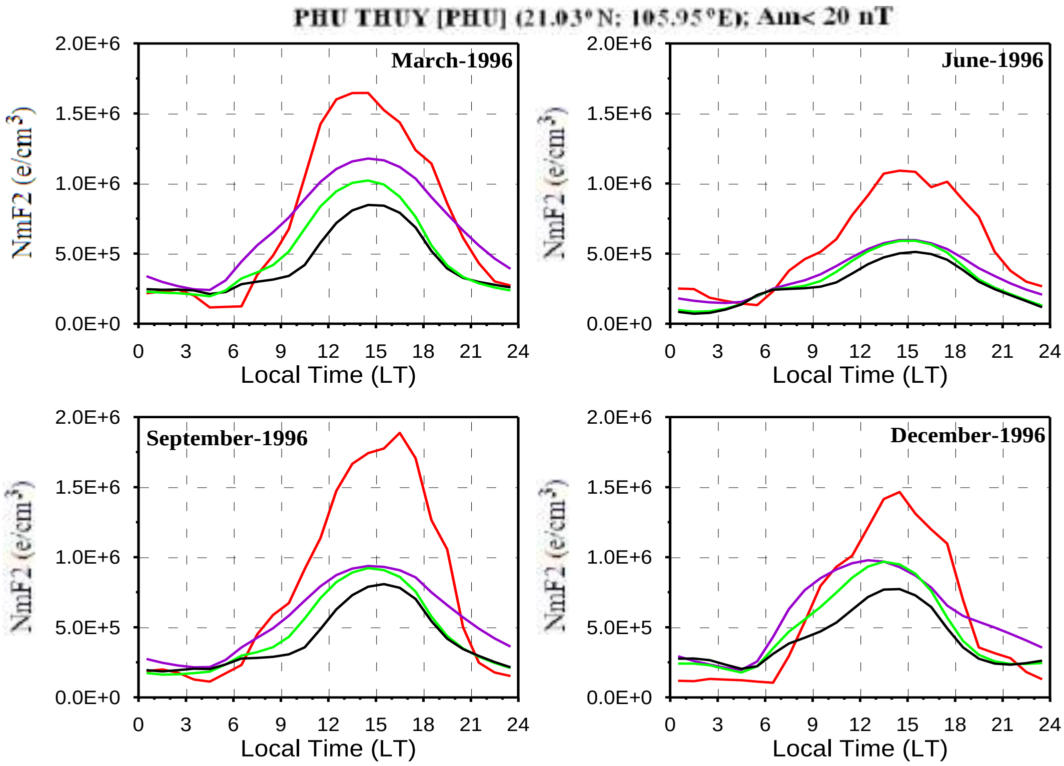

Figure 4. Sames as Figure 3 but for 1996

3.3. Simulation in the geomagnetic perturbation

Geomagnetic activity is a manifestation and measure of “space weather”, arising from the interaction between the solar wind and the Earth’s magnetosphere. This interaction generates currents in the ionosphere and magnetosphere which cause perturbations in the main magnetic field of the Earth that can be measured at the surface. These magnetic perturbations form the basis of indices of geomagnetic activity, such as the Ap, aa, and Kp indices. Each of these indices is derived from the K index, which is related to the maximum fluctuations of the horizontal components of the observed geomagnetic field during a three-hour interval. Figure 5 shows, from the top to the bottom, the time variations of aa, am, Kp and Dst indices as a function of UT time from 25 March to 3 April 2008. The variations of the aa, am and Kp indices are similar. Around 2100 UT on 25 March these indices change suddenly and reach a first maximum about 0400 UT on 26 March, then fluctuate to reach a second maximum around 0400 UT on 27 March during the main phase of the storm. The indices then decrease gradually to the normal level on 3 April in the recovery phase of the storm. The Dst index decreases from the maximum of +14 nT on 26 March to the minimum of -56 nT at the midnight on 27 March (main phase), then it increases gradually in the recovery phase to reach the normal level on 3 April.

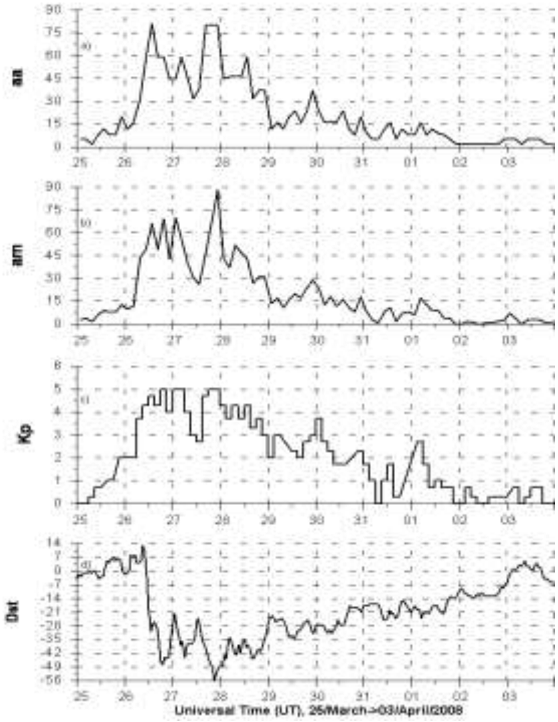

Figure 5. Geomagnetic and solar indices: a) aa index, b) am index, c) Kp index, d) Dst index, as a function of UT time, from 25 March to 3 April 2008

Figure 6 illustrates the variation of the horizontal component H of the Earth's magnetic field observed at Phu Thuy from the mentioned period. The geomagnetic storm is clearly visible on this figure. The first phase of the storm lasts from 21.00 UT on 25 March to 04.00 UT on 26 March; the main phase lasts from 04.00 UT on 26 March to 22.00 UT on 27 March. The recovery phase of the storm begins at 22.00 UT on 27 March and ends on about 3 April.

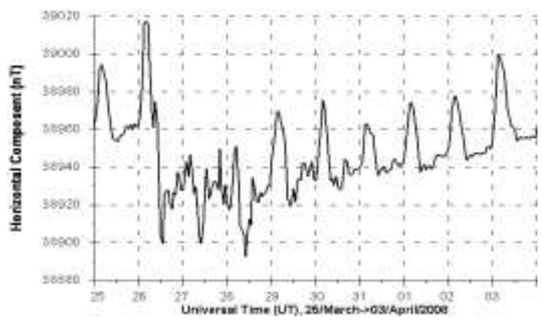

Figure 6. The variation of the horizontal component H of the Earth's magnetic field observed at Phu Thuy from 25 March to 03 April 2008

Figure 7 presents the simulated f_0F_2 (top panel) and the observed NmF2 (bottom panel) during this geomagnetic storm (simulation $n^0 6$). The decrease of the maximum electron density is observed especially during the night of the 27 March. The change of the maximum electron density (NmF2) seems to be greatest at the end of the main phase of the storm (more than one day after the beginning of the main phase).

According to Huang et al., (1989), the state of the ionosphere near the crest of equatorial anomaly during geomagnetic storms is dominated by two processes: the neutral wind meridian and change of the neutral gas components.

During magnetic storms, an enhancement of the auroral Joule heating by auroral phenomena in the upper atmosphere can affect the meridional wind circulation in the F2- region from the pole to the equator. These winds produce disturbances of ionospheric electric fields and currents. This mechanism is called the ionospheric disturbance dynamo, and built up by Blanc and Richmond (Blanc and Richmond, 1980).

This wind will increase the ionization along the lines of Earth's magnetic field at higher altitudes. A decrease of the electron density of the F2- layer can appear associated an increase of neutral molecules of N_2 and O_2. The increase of N_2 and O_2 densities will cause the reduction of the ratio of the N-N_2 and O-O_2, and also the increase of electron-ion recombination rate, resulting in reduction of the electron density NmF2.

Figure 7 below shows a strong decrease of NmF2 on 27 March. This is due to the storm wind between the equator and the pole which takes a few hours to reach the equator and could be maintained for several days after the end of the storm. The decrease of NmF2 is related to the meridional wind between the pole and the equator.

On the figure 6, we can clearly see the effect of Dst as well as the regular daily variation S_R in the H component. The regular variation S_R is very weak on 27 and 28 March, this is the signature of the ionospheric disturbance dynamo (Le Huy M. et al., 2005, 2008). This mechanism generates an anti-Sq type of current vortex is added to the S_q current, and we observe a reduction of the S_q current.

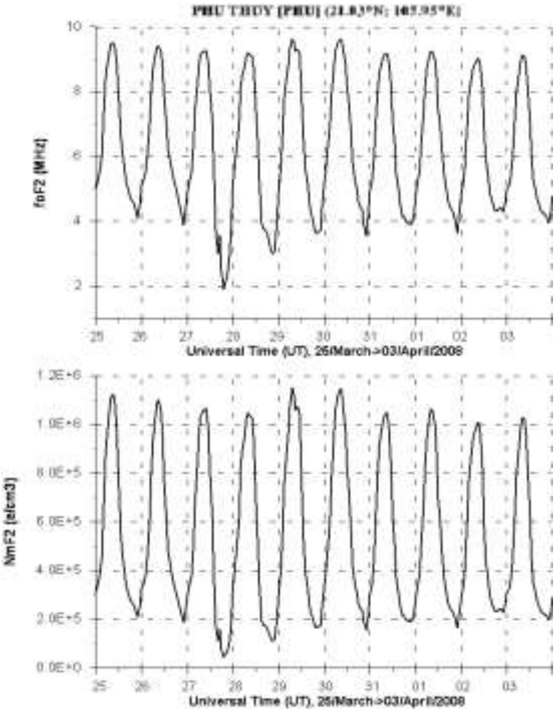

Figure 7. The f_0F_2 (top panel) and the NmF2 (bottom panel) during geomagnetic storm from 25 March to 03 April 2008

4. Conclusion

The analysis of the variation of simulated f_0F_2 by the TIE-GCM shows that this model reproduces some features of f_0F_2. It reproduces well the variation f_0F_2 as a function of local time and the seasonal variation. We found that the variation of the simulated f_0F_2 reproduces the variation observed at the observatory Phu Thuy in 1964. On the contrary, the TIE-GCM does not reproduce the observed amplitude at Phu Thuy in 1996. The TIE-GCM with the chosen inputs does not yet allow us to explain well the long-term variations observed at Phu Thuy.

We also try the different numerical simulations in order to understand how the long-term variations of the f_0F_2 is formed and how it is related to the current global system and to the thermospheric wind. These results show that the simulated NmF2 values are lower than the observed values. In addition, the simulations showed that the modeled contributions of the migrating and non-migrating diurnal and semidiurnal tides play a major role in reducing the amplitude of the NmF2. The contributions of the integrated hemispheric power of auroral electrons and the cross polar cap potential seem to play an important role in increasing the amplitude of the NmF2.

The differences between some of the details of the TIE-GCM predictions and observations indicate that the model and its inputs can be further improved. For example, amplitude, phase, and distribution of the tides, or distribution of the integrated hemispheric power of auroral electrons and the cross polar cap potential in the TIE-GCM which affect the variation of NmF2 can be improved. This work shows also that the variation of NmF2 depends on effects in the dynamo E-region.

Acknowledgements

This research is funded by Vietnam National Foundation for Science and Technology Development (NAFOSTED) under grant number 105.05-2014.30. The authors thank the NGDC data centre for the basis of indices of geomagnetic activity. The authors thank Arthur D. Richmond in the High Altitude Observatory, National Center for Atmospheric Research, Boulder, Colorado, USA to give many indications for using TIE-GCM to analyze ionospheric data.

References

Aikin, A.C., Chanin, M.L., Nash, J., Kendig, D.J., 1991: Temperature trends in the lower mesosphere, Geophys. Res. Let., 18 (3), 416-419.

Blanc, M., Richmond, A.D., 1980: The ionospheric disturbance dynamo, J. Geophys. Res., 85, 1669.

Clilverd, M.A., Clark, T.D.G., Clarke, E., Rishbeth, H., 1998: Increased magnetic storm activity from 1868 to 1995, J. Atmos. Solar-Terr. Phys., Vol. 60, pp. 1047-1056.

Cnossen, I., Richmond, A.D., Wiltberger, M., Wang, W., Schmitt, P., 2011: The response of the coupled magnetosphere-ionosphere-thermosphere system to a 25% reduction in the dipole moment of the Earth's magnetic field, J. Geophys. Res., in press.

Elias, A.G., de Artigas, M.Z., de Haro Barbas, B.F., 2010: Trends in the solar quiet geomagnetic field variation linked to the Earth's magnetic field secular variation and increasing concentrations of greenhouse gases, J. Geophys. Res., Vol. 115, No. 8, A08316, doi: 10.1029/2009JA015136.

Hagan M.E. Forbes, J.M., 2002: Migrating and non migrating diurnal tides in the middle and upper atmosphere excited by tropospheric latent heat release, J. Geophys. Res., 107, D24, 4754.

Hagan M.E., Forbes, J.M., 2003: Migrating and non migrating semidiurnal tides in the upper atmosphere excited by tropospheric latent heat release, J. Geophys. Res., 108, A2, 1062.

Heelis, R.A., Lowell, J.K.,, Spiro, R.W., 1982: A model of the high-latitude ionospheric convection pattern, J. Geophys. Res., 87, 6339-6345.

Huang, Y.-N., Cheng, K., Chen, S.-W, 1989: On the equatorial anomaly of the ionospheric total electron content near the northern anomaly crest region, J. Geophys. Res.: Space physics 94 (A10), 13515–13525.

Jarvis, M.J., Jenkins, B., Rodgers, G.A., 1998: Southern hermisphere observations of a long-term decrease in F region altitude and thermospheric wind providing possible evidence for global thermospheric cooling, J. Geophys. Res., 103 (A9), 20775-20778.

Le Huy M., Amory-Mazaudier C., 2005: Magnetic signature of the ionospheric disturbance dynamo at equatorial latitudes: ‘‘Ddyn’’, J. Geophys. Res., vol. 110, A10301, doi:10.1029/2004JA010578.

Le Huy M., Amory-Mazaudier C., 2008: Planetary magnetic signature of the storm wind disturbance dynamo currents: Ddyn, J. Geophys. Res., vol. 113, A02312, doi:10.1029/2007JA012686.

Macmillan, S., Droujinina, A., 2007: Long-term trends in geomagnetic daily variation, Earth Planets Space, Vol. 59, pp. 391-195.

Menvielle M., Berthelier, A., 1992: The K-derived planetary indices: description and availability, Geophys. Space Phys., 30, 91.

Menvielle M., Marchaudon, A., 2006: Geomagnetic indices, in Solar-Terrestrial Physics and Space Weather in Space Weather, J. Lilensten (ed), Spr., 277-288, 2006.

Menvielle M., Iyemori, T., Marchaudon, A., Nosé, M., 2011: Geomagnetic indices, in Geomagnetic Observations and Models, M. Mandea, M. Korte (eds), IAGA Special Sopron Book Series 5, DOI 10.1007/978-90-481-9858-0_8, Spr.

Pham Thi Thu, H., Amory-Mazaudier, C., Le Huy M., 2011: Time variations of the Ionosphere at the northern tropical crest of ionization at Phu Thuy-Vietnam, Ann. Geophys., 29, pp. 197-297.

Quian, L., Burns, A.G., Solomon, S.C., Roble, R.G., 2009: The effect of carbon dioxide cooling on trends in the F2-layer ionosphere, J. Atmos. Solar-Terr. Phys., Vol. 71, pp. 1592-1601.

Richmond, A.D., Ridley, E.C., Roble, R.G., 1992: A thermosphere/ ionosphere general circulation model with coupled electrodynamics, Geophys. Res. Let., 19(6), 601-604.

Richmond, A.D., 1995: Ionospheric electrodynamics using Magnetic Apex coordinates, J. Geomagn. Geoelectr., 47, 191-212.

Rishbeth, H., Garriott, O.K., 1969: Introduction to Ionospheric Physics, International Geophysics series, Acad. Pres., New York and London, volume 14.

Roble, R.G., 1995: Major greenhouse cooling (yes, cooling): The upper atmosphere response to increased CO_2, Reviews of Geophysics, 33, 539-546.

Stamper, R., Lockwood, M., Wild, M. N, Clark, T.D.G., 1999: Solar causes of the long-term increase in geomagnetic activity, J. Geophys. Res., Vol. 104, pp. 28325-28342.

Ulich, T., Turunen, E., 1997: Evidence for long-term cooling of the upper atmosphere in ionosonde data, Geophys. Res. Let., 24(9), 1103-1106.